3156 *Biochemistry* **2010,** *49,* 3156–3160
DOI: 10.1021/bi1000239

BIOCHEMISTRY
including biophysical chemistry & molecular biology
Article

An Exposed Cysteine Residue of Human Angiostatic Mini Tryptophanyl-tRNA Synthetase[†]

Keisuke Wakasugi*

Department of Life Sciences, Graduate School of Arts and Sciences, The University of Tokyo, 3-8-1 Komaba, Meguro-ku, Tokyo 153-8902, Japan, and PRESTO, Japan Science and Technology (JST), 4-1-8 Honcho, Kawaguchi, Saitama 332-0012, Japan

Received January 7, 2010; Revised Manuscript Received March 9, 2010

ABSTRACT: Human tryptophanyl-tRNA synthetase (TrpRS) catalyzes the aminoacylation of $tRNA^{Trp}$. Human TrpRS exists in two forms: a major form that is the full-length protein and a truncated form (mini TrpRS) in which most of the N-terminal extension is absent. Human mini, but not full-length, TrpRS has angiostatic activity. Because the full-length protein, which lacks angiostatic activity, has all of the amino acid determinants of the mini form, which has activity, I searched for conformational differences between the two proteins. Using a disulfide cross-linking assay, I showed that the molecular environment around Cys62 is significantly different between the two proteins. This difference can be explained by inspection of the three-dimensional structure of the full-length protein. These results give a clear demonstration of a significant difference, around a specific residue (Cys62), between a potent angiostatic and nonangiostatic version of human TrpRS.

Aminoacyl-tRNA synthetases are key enzymes in the process of protein biosynthesis and catalyze the aminoacylation of their cognate tRNAs (*1*). Human tryptophanyl-tRNA synthetase (TrpRS)[1] participates in protein synthesis and angiogenic signal transduction pathways (*2*−*4*). Mammalian TrpRSs contain an additional domain at the N-terminus that is absent from lower eukaryotic and prokaryotic TrpRSs (*5*). In human cells, TrpRS exists in two forms: a major form that is the full-length protein (amino acids 1−471) and a truncated form (mini TrpRS) (amino acids 48−471) in which most of the N-terminal extension (amino acids 1−47) is absent because of alternative splicing of the pre-mRNA (Figure 1) (*5*−*8*). Proteolytic digestion of human full-length TrpRS with the extracellular protease leukocyte elastase produces an additional N-terminally truncated form, T1 TrpRS (amino acids 71−471) (Figure 1) (*2*). Human full-length, mini, and T1 TrpRSs can catalyze the aminoacylation of $tRNA^{Trp}$ (*2*, *9*). Human mini and T1 TrpRSs exhibit angiostatic activity, whereas the full-length enzyme does not (*2*).

The level of expression of human TrpRS is strongly increased in response to interferon-γ (IFN-γ) (*8*, *10*, *11*). TrpRS is the only aminoacyl-tRNA synthetase whose expression is induced by IFN-γ. My previous study established that human full-length TrpRS binds Zn^{2+} or an iron protoporphyrin IX complex (heme), which enhances its aminoacylation activity (*12*). Recently, I reported that human full-length H130R TrpRS is constitutively active and that its aminoacylation activity is not dependent upon the presence of Zn^{2+} or ferriprotoporphyrin IX chloride (hemin) (*13*).

In this study, I investigate whether the human mini H130R TrpRS exhibits the same constitutive activity as the human full-length H130R enzyme. Moreover, I show that the human mini, but not full-length, H130R TrpRS mutant forms disulfide bonds and that there are additional functional differences between the human full-length and mini TrpRSs.

EXPERIMENTAL PROCEDURES

Chemicals. Brewer's yeast tRNA was purchased from Roche Diagnostics (Basel, Switzerland).

Preparation of Proteins. cDNA fragments of human full-length TrpRS (amino acids 1−471), human mini TrpRS (amino acids 48−471), and human T1 TrpRS (amino acids 71−471) were separately cloned into the pET20b (Novagen, Madison, WI) expression vector to give a gene product with a C-terminal tag of six histidine residues (six-His tag). A QuikChange site-directed mutagenesis system (Stratagene, La Jolla, CA) was used to introduce substitutions at specific sites. The final constructs were confirmed by DNA sequencing (FASMAC Co., Ltd., DNA sequencing services, Atsugi, Japan) to ensure no mistakes had been introduced during amplification. The expression constructs were introduced into *Escherichia coli* BL21(DE3) (Novagen). The cells were grown at 37 °C to an OD_{600} of approximately 0.8, and then heterologous gene expression was induced by the addition of 0.4 mM isopropyl β-D-thiogalactopyranoside (IPTG). Cells were harvested 4 h after induction. Using the procedures described by Novagen, the recombinant six-His-tagged proteins were purified on a nickel affinity column (His·Bind resin, Novagen) from the supernatant of lysed cells.

After purification, recombinant TrpRS proteins were dialyzed against 50 mM Tris-HCl (pH 7.5) containing 10 mM EDTA for 1 day. EDTA was subsequently removed from the solution by further dialysis. Protein concentrations were determined by the

[†]This work was supported in part by the Astellas Foundation for Research on Metabolic Disorders, the Kato Memorial Bioscience Foundation, the Takeda Science Foundation, and Grant-in-Aid 21570129 for Scientific Research (C) from the Ministry of Education, Culture, Sports, Science and Technology of Japan.

*To whom correspondence should be addressed. Phone: 81-3-5454-4392. Fax: 81-3-5454-4392. E-mail: wakasugi@bio.c.u-tokyo.ac.jp.

[1]Abbreviations: TrpRS, tryptophanyl-tRNA synthetase; hemin, ferriprotoporphyrin IX chloride; PBS, phosphate-buffered saline; DTT, dithiothreitol; SDS−PAGE, sodium dodecyl sulfate−polyacrylamide gel electrophoresis.

 Published on Web 03/12/2010

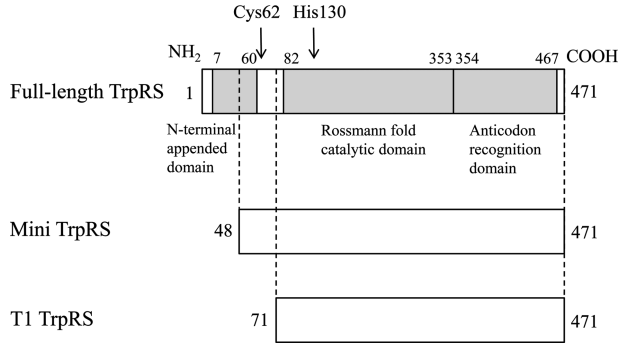

FIGURE 1: Schematic representation of human TrpRS constructs used in this study. Numbers on the left and right correspond to the NH_2- and COOH-terminal residues, respectively, relative to the human full-length TrpRS. Human TrpRS forms a dimer. In one monomer of the dimer, all three domains of human TrpRS [N-terminal appended domain (amino acids 7−60), Rossmann fold catalytic domain (amino acids 82−353), and anticodon recognition domain (amino acids 354−467)] were resolved (*16*). A disordered region of 21 residues (61−81) is likely to be a flexible linker between the N-terminal appended domain and the Rossmann fold catalytic domain. In the other monomer, the first 96 residues, which include the N-terminal appended domain, the flexible linker, and part of the Rossmann fold catalytic unit, were completely disordered (*16*).

Bradford assay using bovine serum albumin (BSA) (Sigma, St. Louis, MO) as the standard (Bio-Rad, Hercules, CA). The hemin concentration was determined spectrophotometrically using an extinction coefficient of 170 mM^{-1} cm^{-1} at 403 nm in 80% dimethyl sulfoxide (*12*).

Atomic Absorption Spectrophotometry. The amounts of Zn^{2+} bound to TrpRS proteins were determined by atomic absorption spectrophotometry using a polarized Zeeman atomic absorption spectrometer, type Z-8100 (Hitachi, Tokyo, Japan).

Aminoacylation Assays. Aminoacylation activity was assayed at ambient temperature (~20 °C) in buffer containing the following: 150 mM Tris-HCl (pH 7.5), 150 mM KCl, 10 mM $MgCl_2$, 4 mM ATP, and 34 μM tryptophan [1 μM [^{3}H]Trp (GE Healthcare, Piscataway, NJ)]. The reactions were initiated via addition of the cell lysates or purified samples (200 nM) to a buffer that included brewer's yeast tRNA (500 μM). Reaction samples were removed and spotted onto Whatman 3MM paper filters. After 1 min, the filter disks were added to cold 5% trichloroacetic acid that included 2 mM Trp. The filters were washed three times in cold 5% trichloroacetic acid and 2 mM Trp, twice in ethanol, and once in ether. The washed filters were then subjected to scintillation counting.

Circular Dichroism (CD) Spectra. CD spectra in the far-UV region were recorded with a spectropolarimeter (J-805, Jasco Co., Tokyo, Japan) at 20 °C. The samples were measured at a concentration of 10 μM in phosphate-buffered saline (PBS). The path length of the cells used for the measurements was 1 mm. The molar ellipticity (degrees squared centimeters per decimole) was determined on a mean residue basis. The α-helix content (f_H) was calculated according to the method of Chen et al. (*14*) with the following equation:

$$f_H = -([\theta]_{222} + 2340)/30300$$

SDS−PAGE and Western Blot Analyses. Extracts of soluble proteins were prepared. Protein samples were resolved by electrophoresis on 10% polyacrylamide−SDS gels. Proteins were electroblotted onto Hybond-P PVDF membranes (GE Healthcare) for 1 h. The membranes were incubated for 1 h with anti-TrpRS monoclonal antibody (clone 3A12, Abnova Co., Taipei, Taiwan) in PBS. After being washed three times with PBS containing 0.1% Tween 20, the membranes were incubated with an HRP-linked sheep anti-mouse Ig (GE Healthcare) for 1 h. The membrane was again washed three times with the buffer, and the proteins were visualized using ECL Western blotting detection reagents (GE Healthcare).

Gel Filtration Chromatography. To measure the molecular sizes of proteins, I performed gel filtration chromatography by using a Superdex 200 HR 10/30 column for the FPLC system (GE Healthcare).

RESULTS AND DISCUSSION

Previously, I reported that human TrpRS is a Zn^{2+}-binding protein and that binding of the protein to Zn^{2+} or heme is indispensable for its aminoacylation activity (*12*). The various recombinant wild-type and H130R TrpRSs were prepared as described in Experimental Procedures and dialyzed for 1 day to generate the fully Zn^{2+}-depleted forms. The molar ratio of Zn^{2+} per TrpRS protein was estimated to be less than 10% by atomic absorption spectrophotometry (data not shown).

I first evaluated the aminoacylation activity of the Zn^{2+}-depleted TrpRSs toward yeast $tRNA^{Trp}$ in the absence or presence of Zn^{2+} or hemin since previous studies have shown that human TrpRS can aminoacylate yeast $tRNA^{Trp}$ both in vitro and in vivo (*9*, *12*, *13*, *15*). Zn^{2+} or hemin enhanced the aminoacylation activity of Zn^{2+}-depleted human mini TrpRS (Figure 2A). Previously, I found that the H130R mutation compromised the ability of human full-length TrpRS to bind heme (*12*). Recently, human full-length H130R TrpRS was found to be constitutively active in a manner independent of the presence of Zn^{2+} or hemin (*13*). As shown in Figure 2A, human mini H130R TrpRS was similarly constitutively active and its aminoacylation activity was also independent of the presence of Zn^{2+} or hemin. Moreover, to examine the effects of the H130R mutation on the structure of the human mini TrpRS, I measured the far-UV CD spectra of human mini wild-type and H130R TrpRSs. As shown in Figure 2B, the CD spectra of human mini H130R TrpRS in the absence or presence of DTT were almost identical to those of the human mini wild-type TrpRS, suggesting that the H130R mutation did not perturb the secondary structure of human mini TrpRS. The α-helical content of human mini H130R in the absence or presence of dithiothreitol (DTT) was estimated to be 30.2 or 31.4%, respectively, which is similar to that of human mini wild-type TrpRS (31.2%).

SDS−PAGE of the various TrpRSs showed that human mini H130R TrpRS forms a dimer and exists as a monomer (Figures 3A,B and 5). Prior treatment of the human mini H130R mutant with a reducing agent, DTT, converted the dimer to the monomeric form (Figures 3A and 5), indicating that human mini H130R TrpRS forms diulfide bonds. In contrast, human full-length H130R TrpRS did not form disulfide bonds (Figure 3A).

The X-ray structural analyses clarified that both human full-length and mini TrpRSs form homodimers (*3*, *4*, *15*). The ability of each TrpRS to associate into a dimer or higher-order multimer was examined by gel filtration over a calibrated FPLC Superdex 200 column. As shown in Figure 4A, human mini H130R TrpRS eluted at fractions corresponding to the dimeric form (~100 kDa) and a high-molecular weight (HMW) multimer (Figure 5). Prior treatment of the mini H130R TrpRS with DTT reduced the level of the HMW multimeric complex and increased the level of the

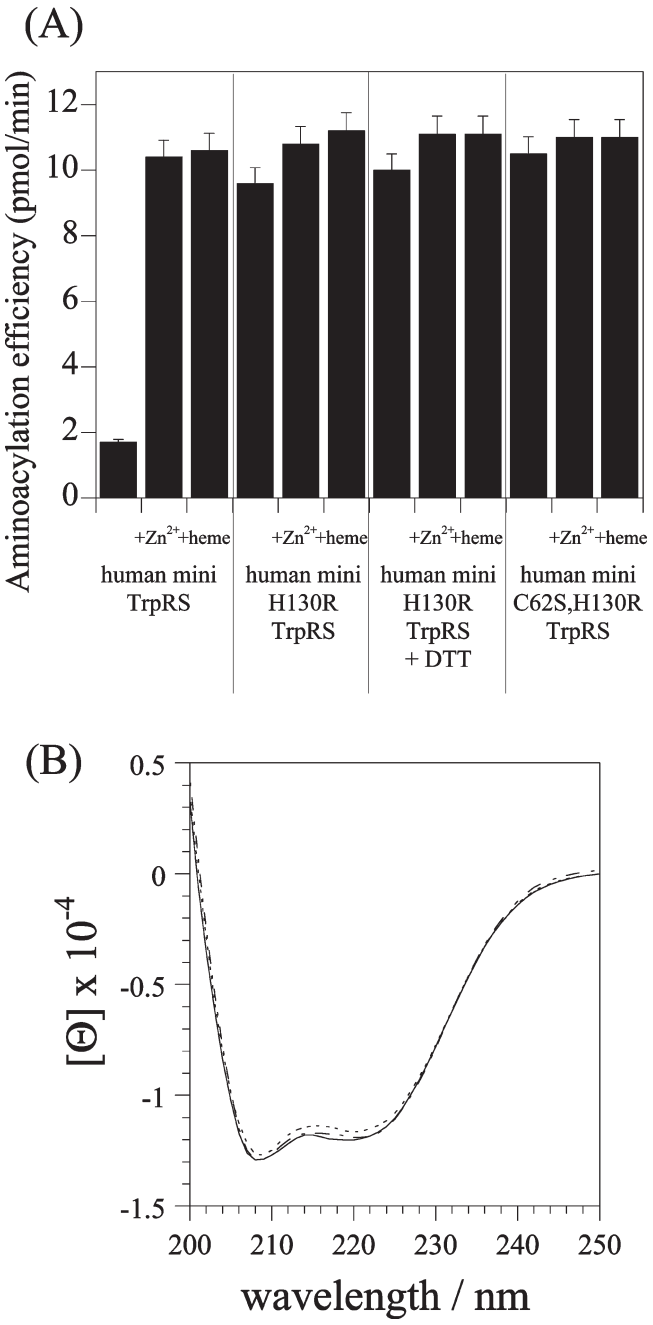

FIGURE 2: Functional and structural analyses of human mini wild-type or H130R TrpRS. (A) Aminoacylation of $tRNA^{Trp}$ by human mini wild-type, H130R, or double mutant (C62S/H130R) TrpRS in the absence or presence of Zn^{2+} (1 μM) or hemin (1 μM). Human mini H130R TrpRS was incubated in the absence or presence of 5 mM DTT for 2 h at 37 °C. Aminoacylation efficiencies were calculated as picomoles of aminoacylated $tRNA^{Trp}$, which was synthesized during a 1 min incubation, per minute. The assays included 200 nM TrpRS and 500 μM yeast tRNA. Values represent means ± the standard deviation from three experiments. (B) Circular dichroism (CD) spectra in the far-UV region of human mini wild-type TrpRS (—) and the human mini H130R mutant in the absence (···) and presence of 5 mM DTT (−·−). The concentration of each TrpRS was 10 μM. Spectra were recorded in phosphate-buffered saline (PBS) at 20 °C.

dimeric complex (Figures 4A and 5), indicating that the human mini H130R forms a HMW disulfide-linked complex.

To delineate the region within the human mini H130R TrpRS that is responsible for formation of disulfide bonds, I prepared a more extensive truncation mutant, human T1 H130R TrpRS.

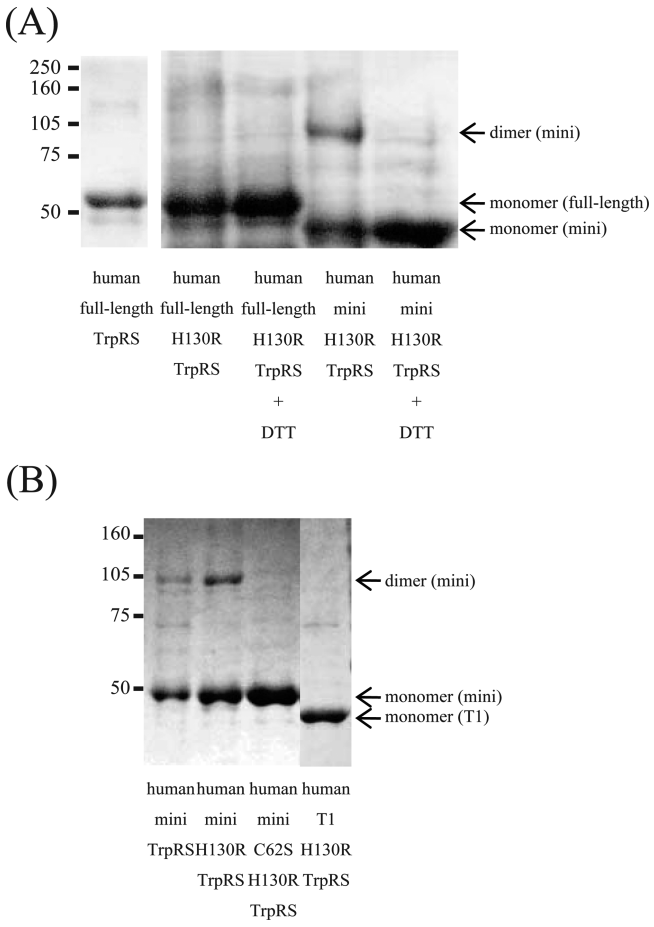

FIGURE 3: SDS−PAGE analyses of human TrpRSs. The samples were analyzed under nonreducing conditions on 10.0% SDS−polyacrylamide gels and stained with Coomassie Blue. Molecular size markers are shown at the left (in kilodaltons). (A) SDS−PAGE analyses of human full-length wild-type or H130R TrpRS, or human mini H130R TrpRS, in the absence or presence of DTT. TrpRS was incubated in the absence or presence of 5 mM DTT for 2 h at 37 °C. (B) SDS−PAGE analyses of human mini wild-type, H130R, double mutant (C62S/H130R), or T1 H130R single mutant TrpRS under nonreducing conditions.

Human T1 TrpRS (amino acids 71−471) is an N-terminally truncated form produced by proteolytic digestion of human full-length TrpRS with the extracellular protease, leukocyte elastase (Figure 1) (*2*). SDS−PAGE analysis showed that human T1 H130R TrpRS does not dimerize (Figure 3B), indicating that it cannot form a disulfide bond. Human full-length and mini TrpRS contain six cysteine residues: Cys62, Cys225, Cys274, Cys305, Cys309, and Cys394 (each residue number is based on the sequence of the full-length form). Since Cys62 exists in the human mini but not T1 TrpRS (Figure 1), I next engineered an H130R mutant TrpRS with the Cys62 residue substituted with Ser. The human mini C62S/H130R double mutant was constitutively active like the human mini H130R TrpRS (Figure 2A). As shown in Figure 3B, the human mini C62S/H130R double mutant did not form disulfide bonds, indicating that Cys62 plays an important role in their formation. Moreover, gel filtration experiments using the human mini C62S/H130R double mutant demonstrated that it largely eluted in a fraction corresponding to the dimer (Figure 4B), suggesting that disulfide bond formation by the human mini H130R TrpRS acts as a seed to facilitate formation of a HMW multimer.

X-ray structural analyses of human full-length and mini TrpRSs showed that a region near Cys62 in the human full-length

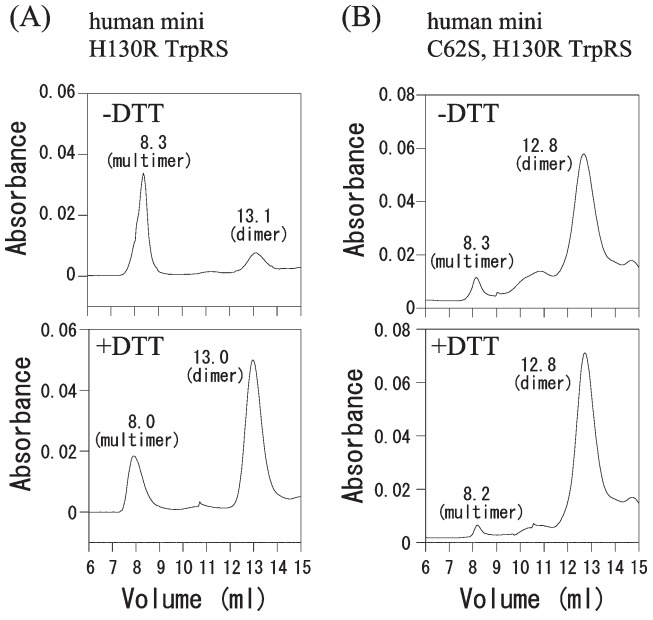

FIGURE 4: Gel filtration chromatography of human mini TrpRS mutants on a Superdex 200 column of the FPLC system. (A) Gel filtration chromatography of human mini H130R TrpRS. Human mini H130R TrpRS was incubated in the absence or presence of 5 mM DTT for 2 h at 37 °C and was loaded onto the column equilibrated with 20 mM Tris-HCl and 150 mM NaCl (pH 7.4) at 4 °C. The optical density profiles were monitored at 280 nm. Elution volumes of blue dextran 2000, ferritin (440 kDa), aldolase (158 kDa), and bovine serum albumin (67 kDa) were 8.3, 10.5, 12.3, and 13.9 mL, respectively, and these data were used for column calibration. (B) Gel filtration chromatography of human mini C62S and the H130R TrpRS double mutant. Human mini double mutant (C62S/H130R) TrpRS was incubated in the absence or presence of 5 mM DTT for 2 h at 37 °C and was injected into the column. Experimental conditions were the same as for panel A.

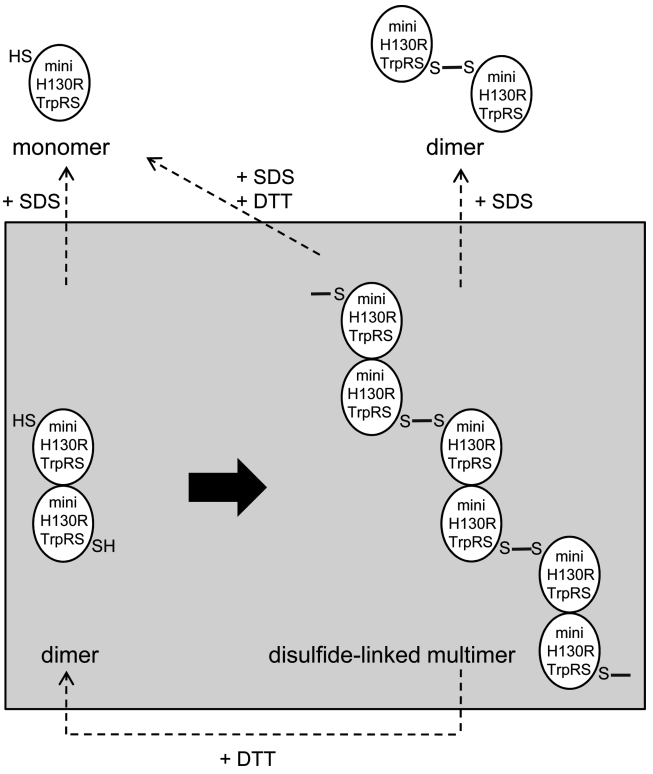

FIGURE 5: Schematic representation of the association properties of human mini H130R TrpRS. Experimental results of SDS−PAGE (Figure 3A,B) and gel filtration chromatography (Figure 4A,B) are summarized. SH and S−S denote a thiol group of a cysteine residue and a disulfide bond, respectively.

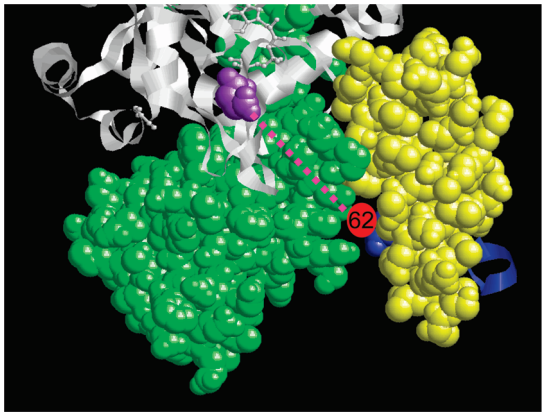

FIGURE 6: Predicted location of Cys62 of human full-length TrpRS. The crystal structure of human full-length TrpRS (Protein Data Bank entry 1R6T) shows that TrpRS consists of an N-terminal appended domain (Ala7−Lys47, yellow space-filling spheres; Met48−Ala60, blue ribbons), a Rossmann fold catalytic domain (Glu82−Ser353, gray ribbons), and an anticodon-binding domain (Asp354−Ala467, green space-filling spheres). Human mini TrpRS lacks the 47 N-terminal residues, which are depicted as yellow space-filling spheres. A disordered region of 21 residues (Asp61−Glu81) is depicted as a magenta dotted line. Ala60 and Glu82 are depicted as blue and purple space-filling spheres, respectively. The predicted position of Cys62 is depicted as a red sphere.

or mini TrpRS is disordered (*3*, *16*, *17*). The disordered region (Asp61−Glu81) of the human full-length TrpRS is located between the N-terminal appended domain and the Rossmann fold catalytic domain (Figure 1). Secondary structure prediction programs suggest that this region lacks any defined secondary structure elements and is likely to adopt a flexible looplike conformation. As shown in Figure 6, the X-ray structure of the human full-length TrpRS suggests that Cys62 of the human full-length TrpRS is buried between the N-terminal appended domain and the anticodon recognition domain. On the other hand, Cys62 of human mini TrpRS would be exposed to solvent due to the lack of the 47 N-terminal residues, which are highlighted in yellow in Figure 6, leading to disulfide formation. These differences between the human full-length and mini TrpRSs are consistent with my results.

As shown in Figure 7, Western blot analyses of human mini wild-type TrpRS demonstrated that human mini TrpRS can form disulfide bonds. However, Figure 3B shows that the extent of disulfide bond formation by human mini wild-type TrpRS is lower than that of human mini H130R TrpRS. Human mini wild-type TrpRS exists in two forms: an enzymatically active Zn^{2+}- or heme-bound form and an inactive Zn^{2+}-depleted form (*12*). On the other hand, the aminoacylation activity of the human mini H130R mutant is not dependent upon the presence of Zn^{2+} or hemin, and this form is constitutively active. These results imply that the enzymatically active human mini TrpRS can form disulfide bonds more easily than the inactive form.

This study has shown that human mini H130R TrpRS tends to form a disulfide bond, leading to the formation of a HMW disulfide-linked multimer. Recently, I reported that an oxidized form of human glyceraldehyde-3-phosphate dehydrogenase (GapDH) interacts with TrpRS and stimulates the aminoacylation activity of the mini, but not full-length, TrpRS (*9*). GapDH is a key redox-sensitive enzyme in glycolysis that catalyzes the NAD-dependent conversion of glyceraldehyde 3-phosphate to

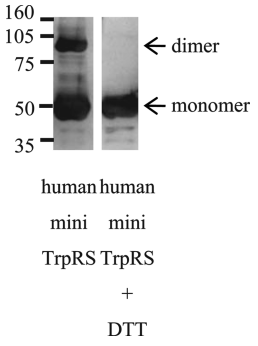

FIGURE 7: Western blot analyses of human mini wild-type TrpRS in the absence or presence of DTT. TrpRS was incubated in the absence or presence of 5 mM DTT for 2 h at 37 °C. Protein samples were analyzed under nonreducing conditions on 10.0% SDS−polyacrylamide gels and by Western blot analysis using an anti-TrpRS mouse monocolonal antibody as described in Experimental Procedures. Molecular size markers (in kilodaltons) are shown at the left.

1,3-diphosphoglycerate. GapDH forms detergent (Triton)-insoluble HMW disulfide-linked multimers following exposure to oxidants, as does the human mini TrpRS (*18*, *19*). Disulfide bonding of GapDH acts a seed to facilitate the misfolding of GapDH, leading to an insoluble conformation and ultimately conversion to a HMW aggregate (*18*). It should be also noted that bovine full-length TrpRS exists in detergent (Triton)-soluble lysates, whereas the detergent-insoluble fraction contained only an approximately 50 kDa polypeptide corresponding to the molecular mass of the mini form (*20*). The production of this detergent-insoluble fraction specific for mini TrpRS may be linked to the formation of disulfide bonds via the active cysteine of mini TrpRS.

Amyloid-β (Aβ) induces disulfide bonding and aggregation of GapDH in Alzheimer's disease (*18*). An increased level of GapDH disulfide bonding is observed in detergent-insoluble extracts from Alzheimer's disease patients compared with age-matched controls (*18*). Long-term exposure of cortical neurons to Aβ resulted in the progressive formation of insoluble disulfide-linked GapDH multimers and large aggregate-like structures in the cytoplasm that were not present in control cells (*18*). Moreover, immunohistochemical analysis of brain sections with antibodies against TrpRS revealed prominent staining of extracellular plaque-like TrpRS aggregates in the hippocampus of Alzheimer's disease brains (*21*). Therefore, further studies are necessary to clarify the relationship between human TrpRS and disease and to investigate novel functions of human TrpRS under oxidative stress conditions, in particular by focusing on posttranslational modification of the exposed cysteine residue, including disulfide bond formation, in human angiostatic mini TrpRS.

REFERENCES

1. Schimmel, P. (1987) Aminoacyl-tRNA synthetases: General scheme of structure-functional relationships in the polypeptides and recognition of transfer RNAs. *Annu. Rev. Biochem. 56*, 125–158.
2. Wakasugi, K., Slike, B. M., Hood, J., Otani, A., Ewalt, K. L., Friedlander, M., Cheresh, D. A., and Schimmel, P. (2002) A human aminoacyl-tRNA synthetase as a regulator of angiogenesis. *Proc. Natl. Acad. Sci. U.S.A. 99*, 173–177.
3. Kise, Y., Lee, S. W., Park, S. G., Fukai, S., Sengoku, T., Ishii, R., Yokoyama, S., Kim, S., and Nureki, O. (2004) A short peptide insertion crucial for angiostatic activity of human tryptophanyl-tRNA synthetase. *Nat. Struct. Mol. Biol. 11*, 149–156.
4. Yang, X.-L., Schimmel, P., and Ewalt, K. L. (2004) Relationship of two human tRNA synthetases used in cell signaling. *Trends Biochem. Sci. 29*, 250–256.
5. Frolova, L. Y., Grigorieva, A. Y., Sudomoina, M. A., and Kisselev, L. L. (1993) The human gene encoding tryptophanyl-tRNA synthetase: Interferon-response elements and exon-intron organization. *Gene 128*, 237–245.
6. Tolstrup, A. B., Bejder, A., Fleckner, J., and Justesen, J. (1995) Transcriptional regulation of the interferon-γ-inducible tryptophanyl-tRNA synthetase includes alternative splicing. *J. Biol. Chem. 270*, 397–403.
7. Turpaev, K. T., Zakhariev, V. M., Sokolova, I. V., Narovlyansky, A. N., Amchenkova, A. M., Justesen, J., and Frolova, L. Y. (1996) Alternative processing of the tryptophanyl-tRNA synthetase mRNA from interferon-treated human cells. *Eur. J. Biochem. 240*, 732–737.
8. Shaw, A. C., Larsen, M. R., Roepstorff, P., Justesen, J., Christiansen, G., and Birkelund, S. (1999) Mapping and identification of interferon γ-regulated HeLa cell proteins separated by immobilized pH gradient two-dimensional gel electrophoresis. *Electrophoresis 20*, 984–993.
9. Wakasugi, K., Nakano, T., and Morishima, I. (2005) Oxidative stress-responsive intracellular regulation specific for the angiostatic form of human tryptophanyl-tRNA synthetase. *Biochemistry 44*, 225–232.
10. Kisselev, L., Frolova, L., and Haenni, A.-L. (1993) Interferon inducibility of mammalian tryptophanyl-tRNA synthetase: New perspectives. *Trends Biochem. Sci. 18*, 263–267.
11. Fleckner, J., Martensen, P. M., Tolstrup, A. B., Kjeldgaard, N. O., and Justesen, J. (1995) Differential regulation of the human, interferon inducible tryptophanyl-tRNA synthetase by various cytokines in cell lines. *Cytokine 7*, 70–77.
12. Wakasugi, K. (2007) Human tryptophanyl-tRNA synthetase binds with heme to enhance its aminoacylation activity. *Biochemistry 46*, 11291–11298.
13. Wakasugi, K. (2010) Species-specific differences in the regulation of the aminoacylation activity of mammalian tryptophanyl-tRNA synthetases. *FEBS Lett. 584*, 229–232.
14. Chen, Y. H., Yang, J. T., and Martinez, H. M. (1972) Determination of the secondary structures of proteins by circular dichroism and optical rotatory dispersion. *Biochemistry 11*, 4120–4131.
15. Johnson, J. D., Spellmann, J. M., White, K. H., Barr, K. K., and John, T. R. (2002) Human tryptophanyl-tRNA synthetase can efficiently complement the *Saccharomyces cerevisiae* homologue, Wrs1P. *FEMS Microbiol. Lett. 216*, 111–115.
16. Yang, X.-L., Otero, F. J., Skene, R. J., McRee, D. E., Schimmel, P., and Ribas de Pouplana, L. (2003) Crystal structures that suggest late development of genetic code components for differentiating aromatic side chains. *Proc. Natl. Acad. Sci. U.S.A. 100*, 15376–15380.
17. Yang, X.-L., Guo, M., Kapoor, M., Ewalt, K. L., Otero, F. J., Skene, R. J., McRee, D. E., and Schimmel, P. (2007) Functional and crystal structure analysis of active site adaptations of a potent anti-angiogenic human tRNA synthetase. *Structure 15*, 793–805.
18. Cumming, R. C., and Schubert, D. (2005) Amyloid-β induces disulfide bonding and aggregation of GAPDH in Alzheimer's disease. *FASEB J. 19*, 2060–2062.
19. Nakajima, H., Amano, W., Fujita, A., Fukuhara, A., Azuma, Y.-T., Hata, F., Inui, T., and Takeuchi, T. (2007) The active site cysteine of the proapoptotic protein glyceraldehyde-3-phosphate dehydrogenase is essential in oxidative stress-induced aggregation and cell death. *J. Biol. Chem. 282*, 26562–26574.
20. Paley, E. L., Baranov, V. N., Alexandrova, N. M., and Kisselev, L. L. (1991) Tryptophanyl-tRNA synthetase in cell lines resistant to tryptophan analogs. *Exp. Cell Res. 195*, 66–78.
21. Paley, E. L., Smelyanski, L., Malinovskii, V., Subbarayan, P. R., Berdichevsky, Y., Posternak, N., Gershoni, J. M., Sokolova, O., and Denisova, G. (2007) Mapping and molecular characterization of novel monoclonal antibodies to conformational epitopes on NH_2 and COOH termini of mammalian tryptophanyl-tRNA synthetase reveal link of the epitopes to aggregation and Alzheimer's disease. *Mol. Immunol. 44*, 541–557.